Ternary and quaternary co-crystals of 1,3-*cis*,5-*cis*-cyclohexanetricarboxylic acid and 4,4′-bipyridines†‡

Balakrishna R. Bhogala and Ashwini Nangia*

Received (in Durham, UK) 8th January 2008, Accepted 11th March 2008
First published as an Advance Article on the web 26th March 2008
DOI: 10.1039/b800293b

1,3*cis*,5*cis*-Cyclohexanetricarboxylic acid (H_3CTA) was co-crystallized with 4,4′-bipyridine bases connected *via* methylene and alkene chains to obtain ternary acid–base co-crystals, H_3CTA·bipy1·bipy2. The hydrogen bond network and mode of interpenetration in co-crystal structures are discussed in relation to known (6,3) nets. The rectangular host container of composition H_3CTA·bipy-eta·(bipy-bu)$_{0.5}$ includes a variety of aromatic guest species in its 10 × 12 Å channels. The ternary and quaternary co-crystals are characterized by X-ray diffraction to analyze the hydrogen bonding and molecular packing. Whereas the acid–pyridine O–H···N hydrogen bond sustains reliable supramolecular aggregation in multi-component crystal structures, the change of bipyridine base connector imparts structural diversity in these supramolecular structures. A self-assembly model based on helix and chain sub-units of acid·bipy1 being connected *via* the bipy2 spacer to give hexagonal and square network structures is proposed.

Introduction

1,3-*cis*,5-*cis*-Cyclohexanetricarboxylic acid (H_3CTA) is a trigonal tecton for the construction of hydrogen-bonded solids, similar to the archetype trimesic acid (1,3,5-benzenetricarboxylic acid, H_3TMA). The better solubility of H_3CTA in common organic solvents and its conformational flexibility due to the cyclohexane ring are favorable factors in exploring structural diversity in co-crystals. We and others have reported binary, ternary and quaternary co-crystals and binary salts of H_3CTA and H_2CTA^- anion with bipyridine and amine bases.[1] There are very few examples of ternary co-crystals to date,[1c,e,2] quaternary co-crystals are even fewer.[1c] We report herein examples of ternary and quaternary solid-state compounds of H_3CTA with different bipyridine bases. For the purpose of this article, we define co-crystals[3] as multi-component solid-state assemblies of two or more compounds held together by any type or combination of intermolecular interactions.[4] Thus, while hydrogen bonding is the most ubiquitous glue to bond co-crystals,[5] other intermolecular interactions such as halogen bonding,[6] π–π stacking,[3a,7] and ion pairing[8] may also be included. The starting components in their pure form are generally solids at ambient conditions[5] but liquid and gaseous states are within the scope of accepted co-crystal definitions.[3,4] The emphasis in this and several other studies is on the use of heterosynthons[9] as design elements to obtain predictable hydrogen bond networks, even as the complete 3D molecular arrangement and crystal packing may be difficult to anticipate. The utility of co-crystals in pharmaceutical formulation and form discovery are discussed elsewhere.[5a,10]

Results and discussion

The molecular components are displayed in Fig. 1. Instead of mixing H_3CTA and one bipyridine base,[1a,b] two bipyridines were co-crystallized with the triacid. The idea was that slight differences in the pyridine N-basicity, hydrogen bond acceptor ability, and close packing groups of these aromatic bases having different connector groups will lead to the incorporation of differentiated bipyridines complexed to the tricarboxylic acid in the solid-state. The selection of bases was based on synthetic accessibility while the stoichiometry of components was decided on the functional groups ratio. We

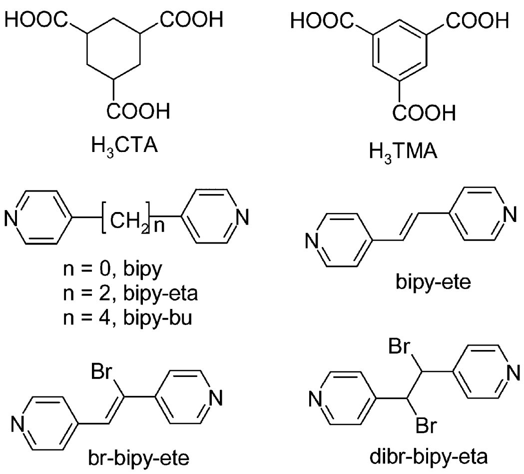

Fig. 1 Carboxylic acid and bipyridine bases used in co-crystallization. Dibr-bipy-eta eliminates HBr *in situ* to give br-bipy-ete for co-crystallization.

School of Chemistry, University of Hyderabad, Hyderabad, 500 046, India. E-mail: ashwini_nangia@rediffmail.com; Tel: +91 40 2550 4231

† Dedicated to Professor Jerry Atwood on the occasion of his 65th birthday.

‡ Electronic supplementary information (ESI) available: Additional packing diagrams, self-assembly scheme for network polymorphs, and synthesis and spectral data of co-crystal structures. CCDC reference numbers 264604–264606 and 681085–681093. For crystallographic data in CIF or other electronic format see DOI: 10.1039/b800293b

Table 1 Crystallographic data on ternary co-crystals **1–4** and quaternary host–guest structures **5a–5h**

	1	**2**	**3**	**4**	**5a**	**5b**	**5c**	**5d**	**5e**	**5f**	**5g**	**5h**
Composition	$H_3CTA\cdot(bipy\text{-}eta)_{0.5}$	$H_3CTA\cdot bipy\text{-}ete\cdot(bipy\text{-}eta)_{0.5}$	$H_3CTA\cdot br\text{-}bipy\text{-}ete\cdot(dibr\text{-}bipy\text{-}eta)_{0.5}$	$H_3CTA\cdot(bipy\text{-}eta)_{0.8}\cdot(br\text{-}bipy\text{-}ete)_{0.2}\cdot(dibr\text{-}bipy\text{-}eta)_{0.5}$	$H_3CTA\cdot bipy\text{-}eta\cdot(bipy\text{-}bu)_{0.5}\cdot(p\text{-}xylene)_{0.5}$	$H_3CTA\cdot bipy\text{-}eta\cdot(bipy\text{-}bu)_{0.5}\cdot(p\text{-}dichlorobenzene)_{0.5}$	$H_3CTA\cdot bipy\text{-}eta\cdot(bipy\text{-}bu)_{0.5}\cdot(o\text{-}xylene)_{0.5}$	$H_3CTA\cdot bipy\text{-}eta\cdot(bipy\text{-}bu)_{0.5}\cdot(o\text{-}chlorotoluene)_{0.5}$	$H_3CTA\cdot bipy\text{-}eta\cdot(bipy\text{-}bu)_{0.5}\cdot(o\text{-}dichlorobenzene)_{0.5}$	$H_3CTA\cdot bipy\text{-}eta\cdot(bipy\text{-}bu)_{0.5}\cdot(p\text{-}anisole)_{0.5}$	$[H_3CTA\cdot bipy\text{-}eta\cdot(bipy\text{-}bu)_{0.5}]_2\cdot(benzyl\ alcohol)$	$[H_3CTA\cdot bipy\text{-}eta\cdot(bipy\text{-}bu)_{0.5}]_2\cdot(bipy\text{-}bu)_{0.5}$
Empirical formula	$(C_9H_{12}O_6)\cdot(C_{10}H_8N_2)\cdot(C_{12}H_{12}N_2)_{0.5}$	$(C_9H_{12}O_6)\cdot(C_{12}H_{10}N_2)\cdot(C_{12}H_{12}N_2)_{0.5}$	$(C_9H_{12}O_6)\cdot(C_{12}H_9BrN_2)\cdot(C_{12}H_{10}Br_2N_2)_{0.5}$	$(C_9H_{12}O_6)\cdot(C_{12}H_{12}N_2)_{0.82}\cdot(C_{12}H_9BrN_2)_{0.18}\cdot(C_{12}H_{10}Br_2N_2)_{0.5}$	$(C_9H_{12}O_6)\cdot(C_{12}H_{12}N_2)\cdot(C_{14}H_{16}N_2)_{0.5}\cdot(C_8H_{10})_{0.5}$	$(C_9H_{12}O_6)\cdot(C_{12}H_{12}N_2)\cdot(C_{14}H_{16}N_2)_{0.5}\cdot(C_6H_4Cl_2)_{0.5}$	$(C_9H_{12}O_6)\cdot(C_{12}H_{12}N_2)\cdot(C_{14}H_{16}N_2)_{0.5}\cdot(C_8H_{10})_{0.5}$	$(C_9H_{12}O_6)\cdot(C_{12}H_{12}N_2)\cdot(C_{14}H_{16}N_2)_{0.5}\cdot(C_7H_7Cl)_{0.5}$	$(C_9H_{12}O_6)\cdot(C_{12}H_{12}N_2)\cdot(C_{14}H_{16}N_2)_{0.5}\cdot(C_6H_4Cl_2)_{0.5}$	$(C_9H_{12}O_6)\cdot(C_{12}H_{12}N_2)\cdot(C_{14}H_{16}N_2)_{0.5}\cdot(C_7H_8O)_{0.5}$	$(C_9H_{12}O_6)_2\cdot(C_{12}H_{12}N_2)_2\cdot(C_{14}H_{16}N_2)\cdot(C_7H_8O)$	$(C_9H_{12}O_6)_2\cdot(C_{12}H_{12}N_2)_2\cdot(C_{14}H_{16}N_2)\cdot(C_{14}H_{16}N_2)_{0.5}$
M_r	464.49	490.52	648.33	585.97	559.65	580.06	559.64	569.85	580.06	563.63	1121.27	1119.28
Crystal system	Monoclinic	Monoclinic	Monoclinic	Monoclinic	Triclinic	Triclinic	Triclinic	Triclinic	Triclinic	Triclinic	Triclinic	Triclinic
Space group	$C2/c$	$P2_1/c$	$P2_1/c$	$P2_1/c$	$P\bar{1}$	$P\bar{1}$	$P\bar{1}$	$P\bar{1}$	$P\bar{1}$	$P\bar{1}$	$P\bar{1}$	$P\bar{1}$
a/Å	33.167(7)	10.5110(14)	11.2591(16)	11.328(3)	5.7110(4)	5.6882(7)	5.7049(6)	5.7053(5)	5.6867(3)	5.7484(5)	5.7311(6)	11.678(2)
b/Å	9.954(2)	11.9877(15)	11.8962(17)	11.837(3)	14.1003(10)	14.0309(18)	14.0883(16)	14.1098(13)	14.0676(8)	14.1360(12)	18.4298(18)	14.124(3)
c/Å	14.988(3)	19.720(3)	20.253(3)	20.015(5)	18.3960(13)	18.390(2)	18.287(2)	18.266(2)	18.354(1)	18.1188(15)	27.577(3)	17.964(3)
α/°	90	90	90	90	86.100(1)	85.767(2)	85.834(2)	86.062(1)	88.400(1)	85.758(1)	94.300(2)	83.231(2)
β/°	110.91(3)	92.511(2)	95.554(3)	94.448(4)	84.560(1)	84.034(2)	82.960(2)	83.130(1)	86.040(1)	83.817(1)	91.509(2)	83.523(2)
γ/°	90	90	90	90	82.123(1)	81.877(2)	82.027(2)	81.920(1)	81.164(1)	81.574(1)	94.623(2)	79.704(2)
Z	8	4	4	4	2	2	2	2	2	2	2	2
V/Å^3	4622.3(19)	2482.4(6)	2700.0(7)	2675.7(12)	1458.51(18)	1442.5(3)	1442.3(3)	1443.4(2)	1447.21(14)	1445.4(2)	2893.6(5)	2882.2(9)
D_c/g cm^{-3}	1.335	1.312	1.595	1.455	1.274	1.335	1.289	1.311	1.330	1.288	1.324	1.206
T/K	298(2)	100	298	298	100(2)	100(2)	100(2)	100(2)	100(2)	100(2)	100(2)	100(2)
F(000)	1960	1036	1308	1205	596	612	596	604	611	596	1217	1046
2θ range/°	2.62–54.98	3.8–52	3.6–52.8	3.6–52	2.92–52.10	2.24–51.46	3–51.6	3–51.4	3.0–52.8	3.0–51.4	2.2–52.0	3.6–52.2
Index ranges	0 to 42 0 to 12 −19 to 18	−12 to 12 −14 to 14 −24 to 24	−14 to 14 −14 to 10 −22 to 25	−13 to 10 −13 to 14 −24 to 24	−7 to 7 17 to 17 −22 to 19	−6 to 6 −17 to 17 −20 to 22	−6 to 6 17 to 17 −22 to 22	−6 to 6 −17 to 17 −22 to 22	−7 to 7 −17 to 17 −22 to 22	−7 to 7 −17 to 17 −22 to 21	−7 to 7 −22 to 22 −34 to 25	−14 to 14 −17 to 17 −19 to 22
N-total	5383	18 168	14 784	15 827	17 524	14 907	20 436	20 347	19 187	9842	22 418	25 927
N-independent	5302	4817	5518	5281	5730	5470	5491	5474	5886	5434	11 350	11 056
N-observed	3011	2753	3475	2500	5007	4327	4462	4431	5179	4473	6965	7843
Parameters	319	346	385	356	383	386	418	427	475	418	812	739
R_1	0.0530	0.1154	0.0475	0.0648	0.0641	0.0479	0.0602	0.0507	0.0579	0.0475	0.1128	0.1707
wR_2	0.1425	0.3229	0.1316	0.1816	0.1637	0.1134	0.1476	0.1389	0.1509	0.1243	0.3377	0.4621
$\Delta\rho_{max/min}$/e Å^{-3}	0.206/−0.202	0.730/−0.309	0.874/−0.475	0.794/−0.450	1.057/−0.448	0.372/−0.386	0.308/−0.238	0.541/−0.411	0.557/−0.610	0.309/−0.210	0.853/−0.607	2.754/−0.585
GOF	1.06	1.03	1.03	1.00	1.04	1.034	1.07	1.04	1.04	1.03	1.03	1.86
Ref.	1*c*	This work	This work	This work	Ref. 1*c*	Ref. 1*c*	This work	This work	This work	This work	This work	This work

obtained ternary interpenetrated (6,3) network structures **1–4** and a ternary host framework **5** of square channels, which included guests to give a family of quaternary host–guest structures **5a–5h**. All co-crystal structures were characterized by X-ray diffraction (Table 1). Preliminary results were communicated previously.[1b,c,e]

$H_3CTA\cdot bipy\cdot(bipy\text{-}eta)_{0.5}$ 1

Co-crystallization of H_3CTA, bipy and bipy-eta from EtOH–benzene in a 2 : 2 : 1 ratio afforded the three-component crystal **1**. The structure of $H_3CTA\cdot bipy\cdot(bipy\text{-}eta)_{0.5}$ in space group $C2/c$ has infinite helices of acid···bipy O–H···N hydrogen bonds (1.69 Å, 177.6°; 1.68 Å, 168.5°; Table 2) along the *b*-axis, and such helices are connected *via* bipy-eta base O–H···N bond (1.62 Å, 167.7°) with the CH_2CH_2 chain lying on the 2-fold axis in the uncommon *gauche* conformation. Hydrogen bonding of H_3CTA with bipy and bipy-eta gave a hexagonal framework of 25 × 32 Å that fills space through triple parallel interpenetration. Fig. 2 shows the acid···bipy-eta synthon connecting triple helices of acid···bipy in the form of a 2D polar layer structure. Helices within a layer have the same handedness and the bipy-eta connector in *gauche* conformation has a single chirality. The crystal structure is centrosymmetric; the inversion center lies between adjacent layers of opposite handedness. The *gauche* conformation of the CH_2CH_2 chain of bipy-eta is perhaps a consequence of achieving efficient close

Table 2 O–H···N Hydrogen bonds (O–H distances neutron normalized to 0.983 Å) in co-crystal structures $H_3CTA\cdot bipy\cdot(bipy\text{-}eta)_{0.5}$ **1**, $H_3CTA\cdot bipy\text{-}ete\cdot(bipy\text{-}eta)_{0.5}$ **2**, $H_3CTA\cdot br\text{-}bipy\text{-}ete\cdot(dibr\text{-}bipy\text{-}eta)_{0.5}$ **3**, $H_3CTA\cdot(bipy\text{-}eta)_{0.8}\cdot(br\text{-}bipy\text{-}ete)_{0.2}\cdot(dibr\text{-}bipy\text{-}eta)_{0.5}$ **4**, $\mathbf{5}\cdot(p\text{-}xylene)_{0.5}$ **5a**, $\mathbf{5}\cdot(p\text{-}dichlorobenzene)_{0.5}$ **5b**, $\mathbf{5}\cdot(o\text{-}xylene)_{0.5}$ **5c**, $\mathbf{5}\cdot(o\text{-}chlorotoluene)_{0.5}$ **5d**, $\mathbf{5}\cdot(o\text{-}dichlorobenzene)_{0.5}$ **5e**, $\mathbf{5}\cdot(anisole)_{0.5}$ **5f** and $(\mathbf{5})_2\cdot$benzyl alcohol **5g**

Co-crystal	D–H···A	D···A/Å	H···A/Å	D–H···A/°
1	O–H···N	2.681(3)	1.69	177.6
	O–H···N	2.655(3)	1.68	168.5
	O–H···N	2.591(3)	1.62	167.7
2	O–H···N	2.620(6)	1.66	166.0
	O–H···N	2.650(6)	1.67	174.2
	O–H···N	2.751(7)	1.78	169.2
3	O–H···N	2.691(6)	1.70	177.7
	O–H···N	2.664(5)	1.68	175.5
	O–H···N	2.693(5)	1.71	174.9
4	O–H···N	2.650(6)	1.77	147.9
	O–H···N	2.682(5)	1.71	170.5
	O–H···N	2.660(5)	1.68	175.2
5a	O–H···N	2.629(3)	1.65	169.1
	O–H···N	2.665(3)	1.68	172.9
	O–H···N	2.652(2)	1.67	176.3
5b	O–H···N	2.637(2)	1.65	173.4
	O–H···N	2.651(2)	1.66	177.0
	O–H···N	2.650(2)	1.66	176.2
5c	O–H···N	2.643(3)	1.67	168.8
	O–H···N	2.664(2)	1.69	171.8
	O–H···N	2.657(2)	1.68	173.
5d	O–H···N	2.636(2)	1.66	169.8
	O–H···N	2.662(2)	1.68	173.0
	O–H···N	2.658(2)	1.68	179.4
5e	O–H···N	2.660(2)	1.69	174.0
	O–H···N	2.664(7)	1.69	169.0
	O–H···N	2.616(2)	1.66	164.7
5f	O–H···N	2.615(2)	1.64	170.5
	O–H···N	2.659(2)	1.68	171.5
	O–H···N	2.661(2)	1.68	172.7
5g	O–H···N	2.655(5)	1.68	172.9
	O–H···N	2.623(5)	1.64	174.5
	O–H···N	2.696(6)	1.73	165.0
	O–H···N	2.601(6)	1.63	167.2
	O–H···N	2.670(5)	1.69	171.5
	O–H···O	2.864(8)	1.97	150.5

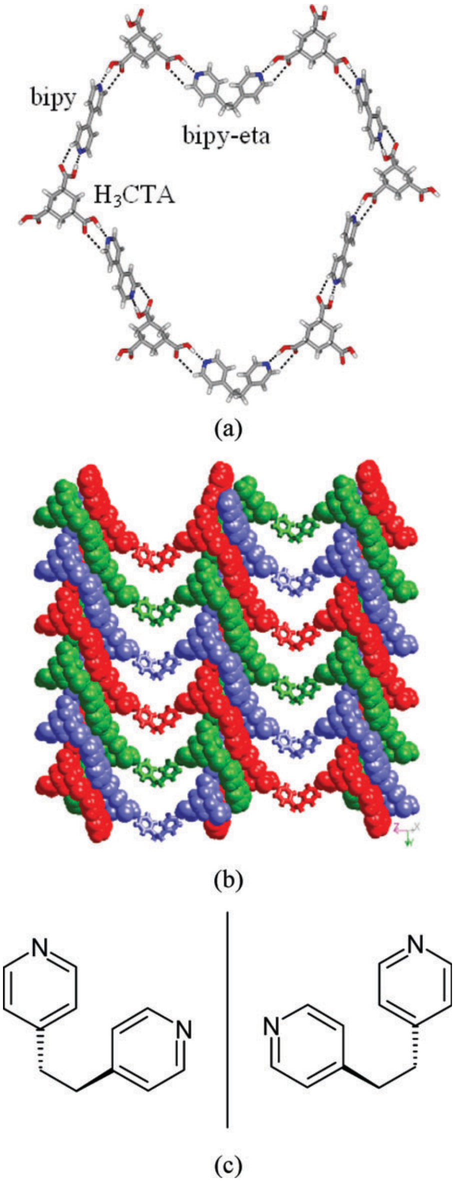

Fig. 2 (a) COOH···bipy and COOH ···bipy-eta heterosynthons assemble in the shape of a molecular necklace of dimensions 25 × 32 Å in crystal structure **1**. (b) The triply interpenetrated (6,3) network showing COOH···bipy helices along [010] and *gauche* CH_2CH_2 connections along [100]. (c) Mirror images of bipy-eta *gauche* chiral conformations in structure **1**.

packing in the region between the helices. The less stable *gauche*-ethylene conformation of bipy-eta is more common in metal–pyridine coordination bonded structures.[11]

The type of interpenetration observed in **1** is a rare variety among the four modes for parallel interpenetration of (6,3) networks reviewed by Batten and Robson (Fig. 3).[12] Zigzag tapes connect to form honeycomb nets in Fig. 3(a), and this kind of interpenetration extends as 2D → 3D parallel interpenetration. Double helices of the same handedness join to give a 2D homochiral network (Fig. 3(b)). Two-fold helices of opposite handedness (*P* and *M*) are arranged alternately to give a centrosymmetric 2D net in Fig. 3(c). Among H_3CTA[1a,b] and H_3TMA[13] network structures, the 2D nets of $H_3CTA\cdot(\text{bipy-eta})_{1.5}$, $H_3TMA\cdot(\text{bipy})_{1.5}$ and $H_3TMA\cdot(\text{bipy-eta})_{1.5}$ interpenetrate in the third mode. Fig. 3(d) shows the connecting 2-fold *M* helices and zigzag tapes alternately.

$H_3CTA\cdot$bipy-ete$\cdot$(bipy-eta)$_{0.5}$ 2

H_3CTA was co-crystallized with bipy-ete and bipy-eta in 2 : 2 : 1 stoichiometry to obtain a ternary co-crystal in which the bipy-ete molecules occupy the helix part and bipy-eta is the connector. ^1H NMR and single-crystal X-ray diffraction ($P2_1/c$ space group) confirmed the formation of $H_3CTA\cdot$bipy-ete$\cdot$(bipy-eta)$_{0.5}$ **2** (see ESI‡ for ^1H NMR data). The asymmetric unit contains one each of H_3CTA and bipy-ete and half molecule of bipy-eta. H_3CTA extends into a helix *via* O–H$\cdots$N hydrogen bond (1.66 Å, 166.0°; 1.78 Å, 169.2°) along the *b*-axis through two acid groups bonded to bipy-ete molecules. These helices connect *via* the third acid group and bipy-eta (O–H$\cdots$N: 1.67 Å, 174.2°) to give a 2D honeycomb motif (Fig. 4). The hexagons of 34 × 36 Å in a single net are filled with two translated nets in the (−3 0 2) plane to produce a triple helix along [010]. In this network *M* and *P* helices are arranged alternately and the mode of interpenetration is similar to Fig. 3(c).

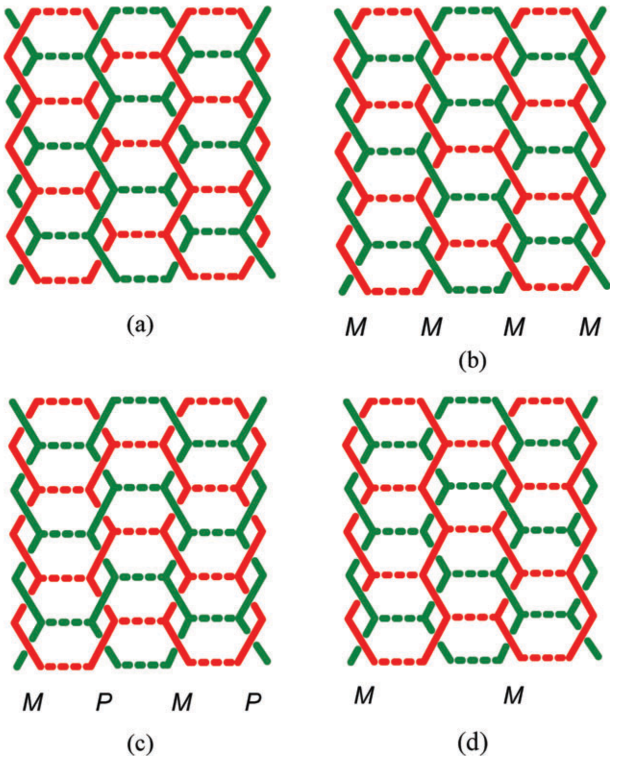

(a) (b) (c) (d)

Fig. 3 Four topologically different modes of parallel interpenetration for (6,3) nets. These modes are analyzed as zigzag tapes and/or helices (solid lines) and connections (broken lines) to give interlocked (6,3) nets. (a) Zigzag tapes, (b) homochiral helices (*M* helices are shown), (c) heterochiral helices (*P* and *M*), (d) helices (*M*) and zigzag tapes alternatively, connect as parallel-interpenetrated honeycomb nets.

$H_3CTA\cdot$br-bipy-ete$\cdot$(dibr-bipy-eta)$_{0.5}$ 3

Co-crystallization of H_3CTA and dibr-bipy-eta in 2 : 3 ratio in EtOH–MeOH at room temperature gave ternary co-crystals of $H_3CTA\cdot$br-bipy-ete$\cdot$(dibr-bipy-eta)$_{0.5}$ **3** as confirmed by ^1H NMR (ESI‡) and single-crystal X-ray diffraction ($P2_1/c$). The co-crystal is ternary in nature because part of the dibr-bipy-eta compound undergoes HBr elimination (promoted by the pyridine base) to produce br-bipy-ete which then becomes a component in co-crystallization (O–H$\cdots$N: 1.70 Å, 177.7°; 1.71 Å, 174.9°). These br-bipy-ete molecules are included between H_3CTA molecules in the helix region and adopt two orientations of equal occupancy. The bromoethylene (CH=CBr) part is disordered as shown in Fig. 5. The helices are joined through dibr-bipy-eta molecules by a O–H$\cdots$N hydrogen bond (1.68 Å, 175.5°) to make honeycomb nets of 32 × 37 Å that are interlocked with two translated nets in the (−3 0 2) plane. In this network structure *M* and *P* helices are arranged alternately similar to Fig. 3(c).

$H_3CTA\cdot$(bipy-eta)$_{0.8}\cdot$(br-bipy-ete)$_{0.2}\cdot$(dibr-bipy-eta)$_{0.5}$ 4

Ternary co-crystallization with a combination of H_3CTA, bipy-eta and dibr-bipy-eta in 2 : 2 : 1 ratio was attempted in MeOH solvent in a deep freezer (4 °C). Diffraction quality crystals were obtained after one week. ^1H NMR of a single crystal (ESI‡) showed the presence of the four components H_3CTA, bipy-eta$\cdot$br, bipy-ete and dibr-bipy-eta in the ratio 1 : 0.8 : 0.2 : 0.5. Single crystal X-ray diffraction ($P2_1/c$) confirmed

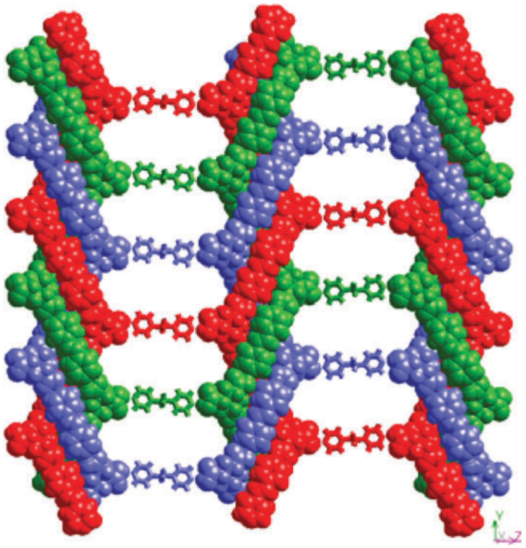

Fig. 4 Three-fold parallel-interpenetration of (6,3) nets in structure **2**. The triple helix of H_3CTA and bipy-ete along [010] is shown as space filling atoms and the bipy-eta connector as cylinder bonds.

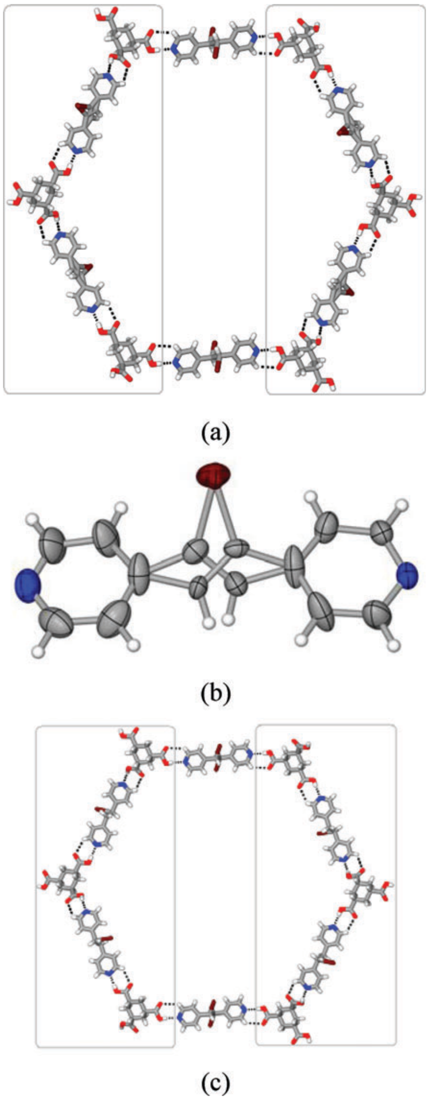

(a)

(b)

(c)

Fig. 5 (a) Helix part (rectangular boxes) of the honeycomb net in **3** formed by H_3CTA·br-bipy-ete which are connected by dibr-bipy-eta. (b) Two orientations of the CH=CBr moiety (s.o.f. 0.5 each) of br-bipy-ete. (c) Helix part (box region) formed by H_3CTA·bipy-eta (s.o.f. 0.82, br-bipy-ete s.o.f. 0.18) and connected *via* dibr-bipy-eta in co-crystal **4**. The 3-fold parallel interpenetrated nets in **3** and **4** are similar to **2**.

the presence of four components in the asymmetric unit: one molecule of H_3CTA, 0.82 molecule of bipy-eta and 0.18 molecule of br-bipy-ete at one occupied site, and half molecule of dibr-bipy-eta. H_3CTA and bipy-eta + br-bipy-ete molecules in 1 : (0.82 + 0.18) ratio form helices (O–H···N 1.77 Å, 147.9°; 1.68 Å, 175.2°) and dibr-bipy-eta molecules joins them to make the 2D honeycomb net (similar to Fig. 5(c)) of 33 × 37 Å dimensions *via* O–H···N hydrogen bonds (1.71 Å, 170.5). The triple parallel interpenetration in **4** is similar to that in Fig. 3(c). Notably ternary structures **2–4** are isomorphous and isostructural to the binary co-crystal H_3CTA·(bipy-eta)$_{1.5}$ prepared earlier.[1b] They crystallized in $P2_1/c$ space group with similar unit cell parameters implying that the C_2 tether plays a space filling role in the crystal structure. However, longer chain length for one of the bipy components gave quite a different crystal structure.

H_3CTA·bipy-eta·(bipy-bu)$_{0.5}$ 5—a three-component host

Co-crystallization with a longer bipy component, such as in H_3CTA, bipy-eta and bipy-bu (2 : 2 : 1), did not afford single crystals from *n*-PrOH and other alcoholic solvents despite several attempts. Upon addition of an aromatic compound to the solution, *e.g.* toluene, *p*-xylene or anisole, diffraction-quality single crystals appeared. The multiple components form ternary host lattice **5** (Fig. 6) for the inclusion of aromatic guests added during crystallization to give host–guest compounds **5a–5h** (Table 1).

The X-ray crystal structure of **5**·*p*-xylene ($P\bar{1}$) confirmed that the aromatic guest is included in the three-component host framework. Two COOH groups of H_3CTA are bonded to different bipy-eta molecules in the *gauche* conformation (O–H···N: 1.65 Å, 169.1°; 1.68 Å, 172.9°), and such dimeric units form square cavities of 10 × 12 Å. These loops are connected *via* O–H···N hydrogen bond (1.67 Å, 176.3°) between the third COOH of H_3CTA and bipy-bu base to give an infinite chain of square loops. Termolecular host containers lying in the plane (0 1 2) stack to form square channels along [100]. The inclusion of *p*-xylene and *p*-dichlorobenzene in the square cavity is shown in Fig. 7.

The construction of a ternary co-crystal host lattice was reported very recently.[1c] Despite being assembled by flexible molecular components, host **5** is structurally robust toward a variety of aromatic guests. Encouraged by the inclusion of *p*-xylene (**5a**) and *o*-dichlorobenzene (**5e**), *p*-dichlorobenzene (mp 53–56 °C) was used as the guest. Since the van der Waals volumes of methyl and chloro substituents are similar (24 and 20 $Å^3$), they can be exchanged in crystal structures without disturbing the crystal packing.[14] The *p*-dichlorobenzene adduct **5b** is a rare example of quaternary co-crystal (four different chemical solids in the same crystal structure)[1c] to be synthesized by deliberate design. The bent conformation of the CH_2CH_2 chain and the wrapping of the host channel around the aromatic guests (Fig. 7) is facilitated by weak hydrophobic host···guest interactions. The chlorine atoms of *p*-dichlorobenzene have s.o.f. 0.81 and 0.19. Partial occupancy of the guest and their orientation/overlap are shown in Fig. 8 and Fig. S1 (see ESI‡), and disorder in host–guest structures is summarized in Table 3.

Network assembly analysis

The assembly of similar molecular components to give hexagonal nets in **1–4** and square loops in **5** may be understood in terms of trigonal tecton at the nodes and bipy connectors. A bottom view of the homochiral net in Fig. 3(b) and heterochiral net in Fig. 3(c) are displayed in Fig. 9. The possible (6,3) networks represent different ways in which helices can build up using the triacid and a bipy base (shown in red and blue) which are connected by the second base (black). Now the finite square loops of **5** are nothing but the helix of **1–4** closing back at the same level (Fig. 9(c)). The connecting group is a homologue bipyridine. In the node and connector representation of Fig. 9, differences in CH_2 chain lengths of bipy bases are ignored and the connector molecules can be bent (gauche conformation) or linear (zigzag conformation). The helix, infinite chain and square box motifs are nothing but

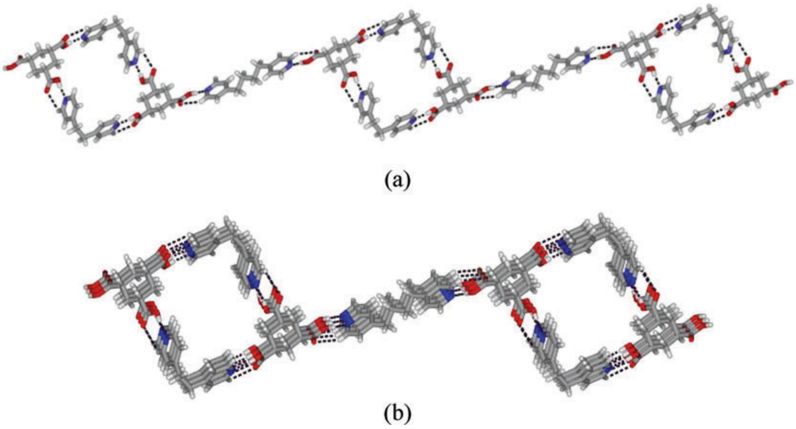

Fig. 6 (a) Closed loop COOH···bipy-eta (*gauche*) units form square boxes which are connected *via* COOH···bipy-bu to form the three-component host **5**. (b) Perfect stacking along [100] to produce square channels of 10 × 12 Å.

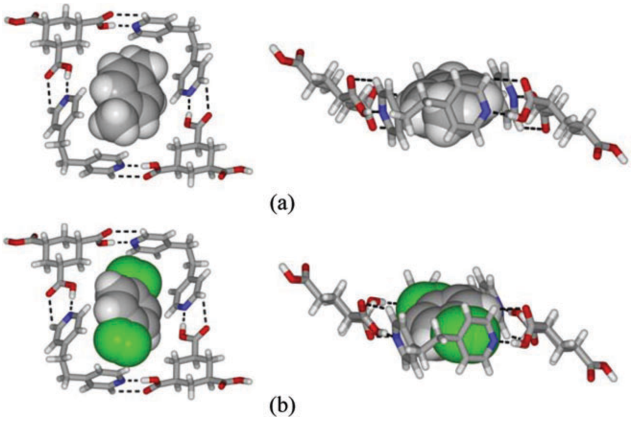

Fig. 7 The orientation and arrangement of guest molecules in the host channel of **5**. (a) *p*-Xylene in **5a** and (b) *p*-dichlorobenzene in **5b** (major occupancy Cl atoms are shown). See Fig. S1 (ESI‡) for guest species in **5c–5f**.

supramolecular isomers.[15] The self-assembly model of Fig. 9 may be used to understand the formation of concomitant network polymorphs of the co-crystal H_3TMA·bipy-eta.[13b] Form II (1 : 1.5) has the usual 3-fold parallel interpenetrated (6,3) net but form I (2 : 3) may be viewed as a chiral (10,3)-*a* net of 18-fold interpenetration. In form II 2_1 triple helices of H_3TMA and bipy-eta join in the 2D layer through bipy-eta and the third acid group. In form I six 4_1 triple helices connect through bipy-eta spacer and the third acid group to give the 18-fold interpenetrated (10,3)-*a* net (Fig. S2, ESI‡). Thus simultaneous formation of 2_1 and 4_1 triple helices from the same building units resulted in concomitant crystallization.

Conclusions

Several examples of ternary co-crystals and quaternary host–guest co-crystals are reported using a combination of H_3CTA and common bipy bases. Crystal structures **1–5** bring

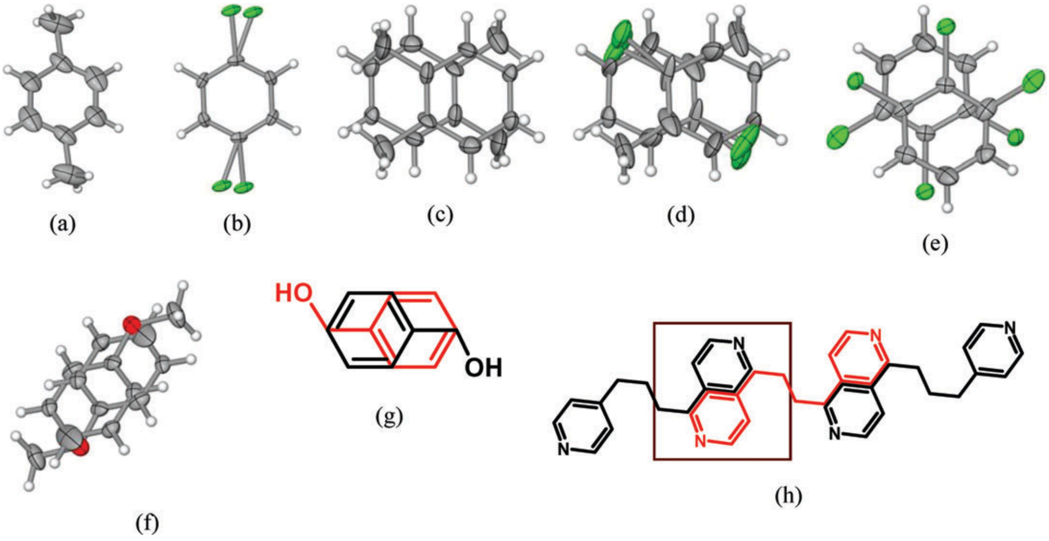

Fig. 8 Guest molecules present in **5a–5h**. Solvent is fully ordered in (a, **5a**) and Cl atoms have s.o.f. of 0.81 and 0.19 in (b, **5b**). Guest disorder is modeled in (c–f, **5c–5f**) about the inversion center. One of the two chlorine atoms in (e) is located on two positions. (g, **5g**) and (h, **5h**) are shown schematically based on the guest electron densities, but atomic positions could not be modeled. In (h) the square box shows a part of the bipy-bu guest in the asymmetric unit.

Table 3 Details of disorder in **5a–5h**

Co-crystal	Guest	**5** : guest ratio in asymmetric unit	Location of the inversion center	Host/guest order/disorder
5a	*p*-Xylene	1 : 0.5	Centre of the square loop	Ordered
5b	*p*-Dichlorobenzene	1 : 0.5	Centre of the square loop	Cl atom disordered
5c	*o*-Xylene	1 : 0.5	Centre of the square loop	Guest disordered
5d	*o*-Chlorotoluene	1 : 0.5	Centre of the square loop	Guest disordered
5e	*o*-Dichlorobenzene	1 : 0.5	Centre of the square loop	Host and guest disordered
5f	Anisole	1 : 0.5	Centre of the square loop	Guest disordered
5g	Benzyl alcohol	2 : 1	Out side the square loop/channel	Host and guest disordered
5h	Bipy-bu	2 : 0.5	Outside the square loop/channel	Host and guest disordered

out simultaneous design strategies for supramolecular construction. (1) The use of a triacid and differentiated bipy bases directs the self-assembly of three components in the solid-state *via* O–H···N hydrogen bonds. (2) The CH_2 chains in bipy bases are not just inert spacers but play a conformational and structural role in directing the supramolecular architecture. This is the first systematic study on the role of CH_2/alkene tethers on the structures of acid–bipy co-crystals.[16] (3) The helix or chain or loop build up of supramolecular structures give hexagonal or square nets from similar starting components. Both achiral and chiral network structures can result from helical aggregates. Why does co-crystallization of a triacid with different bipy base homologs produce ternary adducts? We believe that helices of acid···bipy molecules are constructed with the small/rigid bipy partner whereas connections between these helices/loops involve the longer/flexible bipy base. A possible reason for this selectivity in sequential aggregation could be that the flexible connector component can adopt a larger number of close packing arrangements between the relatively rigid and initially formed acid–bipy helices or chains. The reverse sequence in which the flexible bipy partner is engaged first with the triacid and the rigid bipy docks later may not be equally favorable for achieving efficient close packing in the final crystal structure. Hydrogen bonds are long-range interactions (r^{-1} to r^{-2}) and hence more significant in the early stages of supramolecular association whereas hydrophobic and aromatic interactions operate at short-range (r^{-5} to r^{-6}) towards the final adjustments in the crystal lattice. Whether such bi- and tri-component systems crystallize hierarchically,[17] *via* the helix/chain subunits

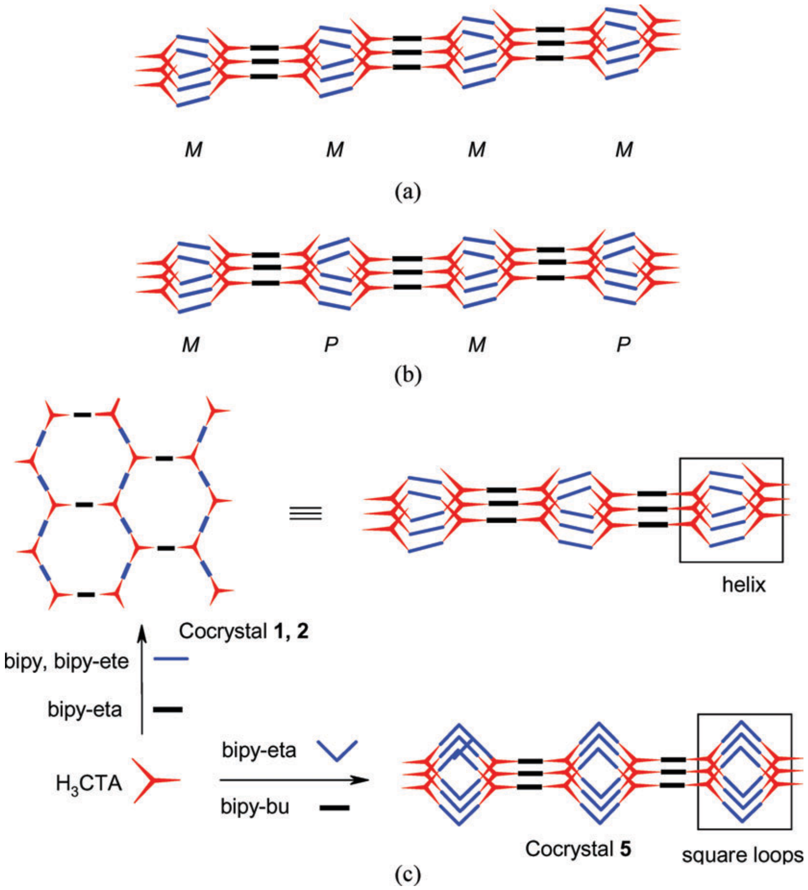

Fig. 9 (a and b) A bottom-side view of homo- and heterochiral (6,3) net in Fig. 3(b) and (c) as a combination of three components in co-crystals **1** and **2**. (c) Formation of hexagonal nets in structure **1** and **2** and square loops in **5** occurs *via* similar molecular components but the difference is in the infinite helix/chain *vs.* closed loop motifs. Molecular component legends are shown by color coding.

forming first followed by connections between the 1D domains to give the final network architecture, is a topic for further investigation. Even as the network assembly of multi-component co-crystals *via* acid···pyridine heterosynthon is well established, the factors that control selective hydrogen bonding with one partner base *vs.* another and the role of methylene and/or alkene tether remain to be fully understood.

Experimental

Synthesis and co-crystallization

Details of all the components used in co-crystallization experiments are given in previous papers[1] except for br-bipy-eta and dibr-bipy-eta. The former was obtained serendipitously in crystallization with dibr-bipy-eta by HBr elimination. Dibromoethane-bipy (dibr-bipy-eta) was prepared using a literature procedure.[18] ^{1}H NMR spectra and co-crystallization procedures are detailed in ESI.‡

X-Ray crystallography

Reflections were collected on Bruker Smart CCD 1000 X-ray diffractometer using Mo-Kα radiation (λ = 0.71073 Å). Details of X-ray data parameters for co-crystals **1** to **5h** are given in Table 1. Intensities were corrected for absorption effects using the multiscan technique SADABS.[19] Structures were solved by the direct methods and refined on F^2 with SHELX-97 and SHELXTL.[20] Non-hydrogen atoms were refined anisotropically in all structures. Acidic hydrogen atoms (OH) in all structures (except **4** and **5e**) were located from difference Fourier maps. All other hydrogen atoms in all the structures bonded to carbon and OH hydrogen atoms in structures **4** and **5e** were fixed in calculated positions. In structure **5h** the hydrogen atoms could not fixed or located because of disorder. Disorder was modeled in all structures except in **5g** and **5h**. Disorder in structures **5** is summarized (Table 3).

Acknowledgements

We thank CSIR (01(2079)/06/EMR-II) for funding. B. R. B. was the recipient of a UGC fellowship. DST (IRPHA) funded the CCD X-ray diffractometer and UGC is thanked for the UPE program.

References

1 (*a*) B. R. Bhogala, P. Vishweshwar and A. Nangia, *Cryst. Growth Des.*, 2002, **2**, 325 (binary); (*b*) B. R. Bhogala and A. Nangia, *Cryst. Growth Des.*, 2003, **3**, 547 (binary, neutral and salts); (*c*) B. R. Bhogala, S. Basavoju and A. Nangia, *Cryst. Growth Des.*, 2005, **5**, 1683 (ternary and quaternary); (*d*) B. R. Bhogala, P. Vishweshwar and A. Nangia, *Cryst. Growth Des.*, 2005, **5**, 1271 (ammonium salts); (*e*) B. R. Bhogala, S. Basavoju and A. Nangia, *CrystEngComm*, 2005, **7**, 551 (binary and ternary); (*f*) B. R. Bhogala and A. Nangia, *Cryst. Growth Des.*, 2006, **6**, 32 (guest influence); (*g*) N. Shan, A. D. Bond and W. Jones, *New J. Chem.*, 2003, **27**, 365 (binary solvate); (*h*) N. Shan, E. Batchelor and W. Jones, *Tetrahedron Lett.*, 2002, **43**, 8721 (binary); (*i*) N. Shan, A. D. Bond and W. Jones, *Cryst. Eng.*, 2002, **5**, 9 (binary).

2 (*a*) T. Smolka, R. Boese and R. Sustmann, *Struct. Chem.*, 1999, **10**, 429; (*b*) C. B. Aakeröy, A. M. Beatty and B. A. Helfrich, *Angew. Chem., Int. Ed.*, 2001, **40**, 3240; (*c*) C. B. Aakeröy, J. Desper and J. F. Urbina, *Chem. Commun.*, 2005, 2820; (*d*) T. Friščić, A. Trask, W. Jones and W. D. S. Motherwell, *Angew. Chem., Int. Ed.*, 2006, **45**, 7546.

3 (*a*) L. S. Reddy, P. M. Bhatt, R. Banerjee, A. Nangia and G. J. Kruger, *Chem.–Asian J.*, 2007, **2**, 505; (*b*) N. J. Babu, L. S. Reddy and A. Nangia, *Mol. Pharmacol.*, 2007, **4**, 417.

4 Similar sentiments are echoed in a recent critique of co-crystal definitions: A. D. Bond, *CrystEngComm*, 2007, **9**, 833.

5 (*a*) Ö. Almarsson and M. J. Zaworotko, *Chem. Commun.*, 2004, 1889; (*b*) C. B. Aakeröy and D. J. Salmon, *CrystEngComm*, 2005, **7**, 439.

6 (*a*) P. Metrangolo, H. Neukirch, T. Pilati and G. Resnati, *Acc. Chem. Res.*, 2005, **38**, 386; (*b*) C. W. Padgett, R. D. Walsh, G. W. Drake, T. W. Hanks and W. T. Pennington, *Cryst. Growth Des.*, 2005, **5**, 745; (*c*) D. Clinčić, Friščić and W. Jones, *Chem.–Eur. J.*, 2008, **14**, 747.

7 (*a*) V. R. Vangala, A. Nangia and V. M. Lynch, *Chem. Commun.*, 2002, 1304; (*b*) L. S. Reddy, A. Nangia and V. M. Lynch, *Cryst. Growth Des.*, 2004, **4**, 89; (*c*) G. W. Coates, A. R. Dunn, L. M. Henling, J. W. Ziller, E. B. Lobkovsky and R. H. Grubbs, *J. Am. Chem. Soc.*, 1998, **120**, 3641.

8 D. Braga and F. Grepioni, *Chem. Commun.*, 2005, 3645.

9 (*a*) L. S. Reddy, N. J. Babu and A. Nangia, *Chem. Commun.*, 2006, 1369; (*b*) A. V. Trask and W. Jones, *Top. Curr. Chem.*, 2005, **254**, 41; (*c*) R. D. B. Walsh, M. W. Bradner, S. Fleischman, L. A. Morales, B. Moulton, N. Rodríguez-Hornedo and M. J. Zaworotko, *Chem. Commun.*, 2003, 186.

10 N. Rodríguez-Hornedo (Editor), Special Section on Pharmaceutical Co-crystals, *Mol. Pharmacol.*, 2007, **4**, 299–434.

11 (*a*) M. Fujita, Y. J. Kwon, M. Miyazawa and K. Ogura, *J. Chem. Soc., Chem. Commun.*, 1994, 1977; (*b*) T. L. Hennigar, D. C. MacQuarrie, P. Losier, R. D. Rogers and M. J. Zaworotko, *Angew. Chem., Int. Ed. Engl.*, 1997, **36**, 972; (*c*) F. M. Tabellion, S. R. Seidel, A. M. Arif and P. J. Stang, *J. Am. Chem. Soc.*, 2001, **123**, 11982.

12 S. R. Batten and R. Robson, *Angew. Chem., Int. Ed.*, 1998, **37**, 1460.

13 (*a*) C. V. K. Sharma and M. J. Zaworotko, *Chem. Commun.*, 1996, 2655; (*b*) T. R. Shattock, P. Vishweshwar, Z. Wang and M. J. Zaworotko, *Cryst. Growth Des.*, 2005, **5**, 2046.

14 J. Chisholm, E. Pidcock, J. van de Streek, L. Infantes, S. Motherwell and F. H. Allen, *CrystEngComm*, 2006, **8**, 11.

15 B. Moulton and M. J. Zaworotko, *Chem. Rev.*, 2001, **101**, 1629.

16 For metal–bipy structures of variable CH_2 chain length, see: M. J. Plater, M. R. St. J. Foreman, T. Gelbrich, S. J. Coles and M. B. Hursthouse, *J. Chem. Soc., Dalton Trans.*, 2000, 3065.

17 C. N. R. Rao, S. Natarajan, A. Choudhury, S. Neeraj and A. A. Ayi, *Acc. Chem. Res.*, 2001, **34**, 80.

18 M. Tanner and A. Ludi, *Chimia*, 1980, **34**, 23.

19 (*a*) *SADABS: Program for Empirical Absorption of Area Detector Data*, ed. G. M. Sheldrick, University of Göttingen, Germany, 1996; (*b*) *Program for Multi-scan Absorption Correction of Area Detector Data*, ed. G. M. Sheldrick, Version 2.10, University of Göttingen, Germany, 2003.

20 (*a*) *SHELX-97: Program for the Solution and Refinement of Crystal Structures*, ed. G. M. Sheldrick, University of Gottingen, Germany, 1997; (*b*) *SHELXTL: Program for the Solution and Refinement of Crystal Structures*, Version 6.12, Bruker AXS Inc., Madison, WI, USA, 2001.